



PRODUCTION AND MECHANICAL PROPERTIES OF GRADIENT MATERIALS BASED ON POLYURETHANES

Cite this: *INEOS OPEN*, **2018**, *1* (1), 58–63
DOI: 10.32931/io1804a

E. S. Afanasyev,^a M. D. Petunova,^a K. S. Piminova,^a G. G. Nikiforova,^a
O. A. Serenko,^a and A. A. Askadskii^{*a,b}

Received 16 March 2018
Accepted 26 April 2018

^a Nesmeyanov Institute of Organoelement Compounds, Russian Academy of Sciences,
ul. Vavilova 28, Moscow, 119991 Russia

^b National Research Moscow State University of Civil Engineering,
Yaroslavskoe shosse 26, Moscow, 129337 Russia

http://ineosopen.org

Abstract

Gradient materials are produced on a unit with programmed control of the speed of feeding of material components into a blender. The materials are derived from 2,4-toluene diisocyanate and poly(propylene glycol). A mixture of dimethylbenzylamine and ED-22 epoxy diene resin is used as a catalyst. The structures and properties of the materials obtained are studied using the following methods: titrimetric definition of the NCO groups, measurement of the refractive index during the reaction, analysis of the hardness, the stress–strain curves and the elasticity modulus. Unlike the products obtained previously on a manually controlled unit, the resulting materials exhibit a gradual change of the elasticity modulus from an elastomer to a solid polymer.

Key words: gradient materials, poly(urethane isocyanurates), elasticity modulus, hardness, refractive index.

Introduction

A unique feature of gradient materials is a gradual change of their properties from a soft rubber to a glassy polymer within one and the same product (sample). Such a control of the hardness, the elasticity modulus and other physico-mechanical characteristics can be achieved only owing to the directed changes in the chemical structure of a polymer matrix during its synthesis, without recourse to the conventional methods for polymer modification or the manual methods for creation of composite structures, such as welding, gluing, or mechanical assembling.

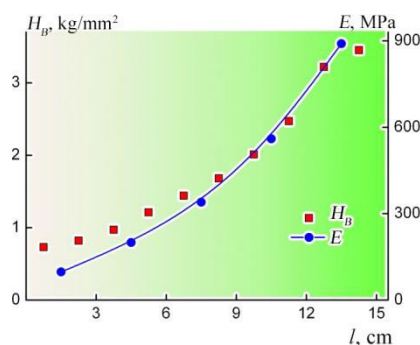
A possibility of production of these materials was predicted theoretically [1–5]. In particular, the material structure must be formed as a dense network containing bulky rigid cross-links connected by flexible chains with controllable lengths. This follows from a generalized equation for evaluation of the equilibrium rubber elasticity modulus E_∞ for network systems, which was derived and described in references [1–5]:

$$E_\infty = E_0 \frac{2(m+\beta)}{\Phi m^2}, \quad (1)$$

where E_0 is the elasticity modulus of a network polymer for which the distance between the network cross-links is comprised by a single repeating unit,

$$E_0 = \frac{3\rho R\Phi T}{2M_0}, \quad (2)$$

m is the number of repeating units in an average fragment between cross-linked points; Φ is the network functionality (the number of chains branching from a cross-link); ρ is the density; R is the universal gas constant; T is the temperature; and M_0 is the molecular mass of the repeating unit in this fragment. The



value of β represents the ratio of the van der Waals volume of the network cross-link $(\sum_i \Delta v_i)_y$ to the van der Waals volume of the repeating unit of a linear fragment $(\sum_i \Delta v_i)_0$

$$\beta = \frac{(\sum_i \Delta v_i)_y}{(\sum_i \Delta v_i)_0} \quad (3)$$

The notion of a network cross-link from the considered viewpoint is described in detail in the above-mentioned references. The network cross-link is a group of atoms which includes an atom serving as a branching center and adjacent chemically bound atoms with their closest substituents.

It can be readily shown that, taking into account formulae (2) and (3), relation (1) goes over into the following equation

$$E_\infty = \frac{3\rho RT}{M_c} \left(1 + \frac{M_0}{M_c}\right), \quad (4)$$

$$\text{or } E_\infty = \frac{3\rho RT}{M_c} \left(1 + \frac{\beta}{m}\right), \quad (5)$$

where M_c is the average molecular mass of the linear fragment between adjacent network cross-links.

If the network is coarse, then $M_c \gg M_0$ and $\beta/m \ll 1$. Under such conditions, equations (4) and (5) go over into the following classical relation

$$E_\infty = \frac{3\rho RT}{M_c} \quad (6)$$

For dense networks, when the distance between adjacent cross-links is equal only to several repeating units or is even shorter than a single unit, the value of β assumes the key role, since $M_c \sim M_0$ and $m \sim 1$. If the process of microphase separation is controlled so that the bulky polar network cross-links form microdomains due to a drastic change of their surface energy from that of the flexible and short nonpolar chains, then these microdomains can serve as network cross-links. In this case the

van der Waals volume of these cross-links, $(\sum_i \Delta v_i)_y$, will essentially exceed that of the repeating unit in the fragments between cross-linked points, $(\sum_i \Delta v_i)_0$, and the value of β , according to equation (3), will acquire higher magnitudes which will lead to the enhanced values of E_∞ according to equations (4) and (5).

Hence, the higher value of E_∞ can be achieved on passing to the dense networks with bulky cross-links, when $M_c \sim M_0$, $m \sim 1$ and $(\sum_i \Delta v_i)_y > (\sum_i \Delta v_i)_0$. It is very important that the elasticity moduli can take on the high values despite the fact the glass-transition point of a polymer network still remains low. This principle was realized in a multitude of works [6–11] by the synthesis of poly(urethane isocyanurate) networks *via* the reaction of polycondensation.

It was mentioned earlier that the production of gradient materials based on network poly(urethane isocyanurates) is a convenient model for realization of their synthesis in an automatic mode using programmed algorithms. Herein we present the results on investigation of the materials obtained on a unit with programmed control of the speed of feeding of material components into a blender. Their gradient structures were confirmed using different physical methods. The properties of the resulting materials were compared to the characteristics of the samples synthesized by the conventional method.

Results and discussion

The samples of the materials obtained on a modified unit do not contain microscopic defects on the surface, are monolithic and uniform, and possess well reproducible properties. Strict control of the speed of feeding of the composition components into a blender allowed us to overcome the drawbacks incident to the samples obtained upon manual control of this parameter of the gradient material synthesis.

Previously it was demonstrated that the gradient material based on PPG-2000 and 2,4-TDI has a network structure, where the bulky network cross-links are formed by the aggregates from isocyanurate rings and the flexible fragments between cross-linked points consist of the poly(propylene glycol) chains. Since the isocyanurate rings possess considerably higher surface energy ($\gamma = 56.8$ mN/m) than PPG-2000 chains ($\gamma = 27.3$ mN/m), the material undergoes microseparation. Its gradient structure is formed by a monotonous change of the number of bulky cross-links in a network structure along the given direction.

Figure 1 shows the stress–strain curves of the samples cut from different zones of the material macrosample according to the diagram presented in Fig. 2. As the content of 2,4-TDI in the composition of a reaction mixture increases and, as a consequence, the content of isocyanurate fragments in a chemical structure of the material grows, there is observed an improvement in the strength characteristics of the microsamples and a change in the form of stress–strain curves. At the minimal content of 2,4-TDI (zones 1, 2), they resemble the stress–strain curves of soft rubbers – the stress monotonously increases with a strain growth. Upon further increase in the concentration of the isocyanurate fragments, the form of the stress–strain curves becomes more typical for rigid rubbers, namely, the stress–strain curves of the samples can be conventionally divided into two

regions with essentially different rates of stress growth upon increase of strain ε . The first region before $\varepsilon \leq 5\%$ corresponds to elastic behavior of the sample; there is observed a linear growth of the stress with a strain rise. Upon further deformation of the sample, the rate of stress growth in it reduces and monotonously increases with a growth in the strain, which is characteristic of dense polymers upon realization in them of rubbery properties. Figure 1b shows the dependence of the stress difference at 30 and 5% deformation of the samples depending on the macrosample length. As the content of the isocyanurate fragments in the material structure increases, the rate of the stress growth in this range of strains firstly increases and then slightly changes while approaching the zones with their highest concentration.

Figure 3 depicts the dependence of the elasticity modulus E on the macrosample length (or an increase in the concentration of the bulky network cross-links). The values of E monotonously increase along the macrosample length as the concentration of 2,4-TDI in the reaction mixture grows. The experimental values of the elasticity modulus fall well on a single dependence which equation has the following form:

$$E = 64.82 + 34.73l - 1.24l^2 + 0.24l^3 \quad (7)$$

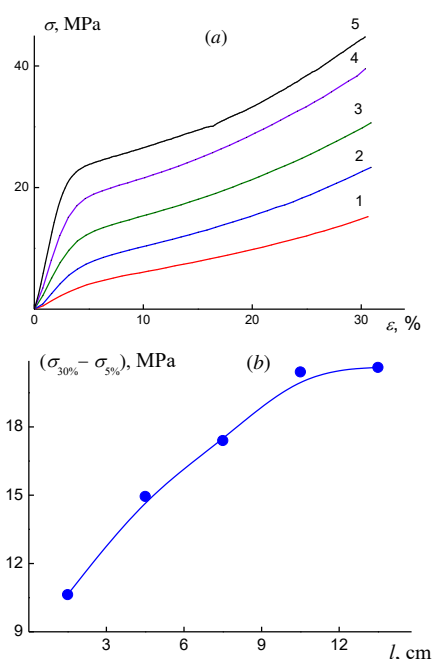


Figure 1. Stress–strain curves of the samples (a) cut from sections 1 (1), 3 (2), 5 (3), 7 (4), and 9 (5) and the dependence of the stress difference at 5 and 30% deformation on the macrosample length (b). The location diagram for the considered macrosample zones is presented in Fig. 2.

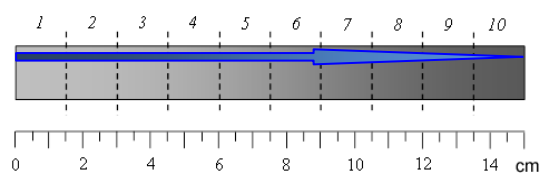


Figure 2. Diagram of cutting of microsamples from the monolithic gradient material. An arrow shows the direction of the growth of 2,4-TDI content in the material sample.

The resulting analytical equation is convenient to use for evaluation of a range of elasticity modulus variation along the

macrosample length. According to relation (7), the value of E at $l \approx 0$ and $l \approx 15$ cm increase in 17 times and compose 65 and 1106 MPa, respectively.

For comparison Fig. 3 shows the values of E for the microsamples cut from the macrosample obtained upon manual control of the speed of feeding of the mixture components [12]. Comparing the experimental values of the elasticity moduli of two gradient materials, one can note that the automatic control of the speed of feeding of the mixture components affords a gradual change of the elasticity moduli of the gradient material, which fall on a single curve. The manual control of the mixing process leads to a number of rises and falls in the elastic modulus growth, which indicates the violation of a monotonous change in the concentration of the isocyanurate fragments along the length of the resulting gradient material.

Figure 4 shows the values of the Brinell hardness number H_B in different zones of the macrosample. The values of H_B , as well as those of the elasticity modulus, monotonously increase with a growth in the content of the isocyanurate fragments along the sample length. For convenience of comparison, Fig. 5 presents the dependences of H_B and E in the same coordinates. As the elastic modulus of the material increases, the rigidity of the microsamples also grows.

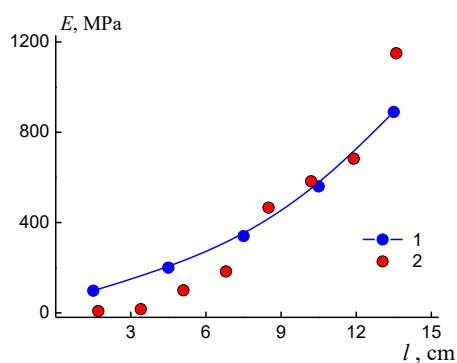


Figure 3. Dependence of the elasticity modulus on the length of the gradient material sample: 1 – material obtained on a modified unit; 2 – material obtained on a unit with manual control of the speed of precursor outflow [12].

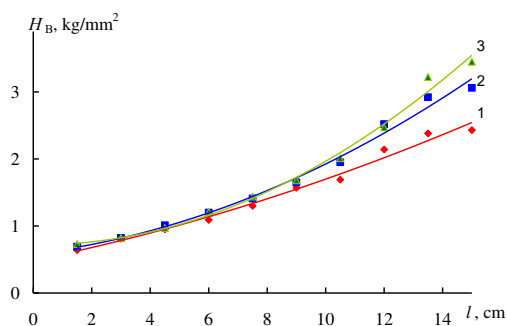


Figure 4. Dependence of the Brinell hardness number on the length of the gradient sample. The loads on the sample were equal to 5 kg (1), 10 kg (2), and 15 kg (3).

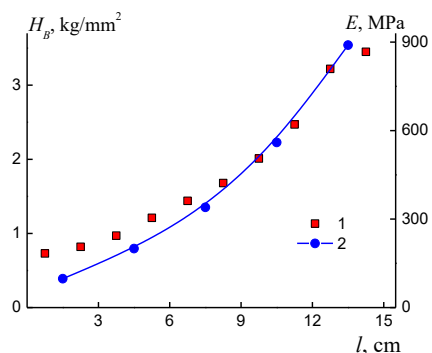


Figure 5. Change in the Brinell hardness number at the load of 15 kg and change in the elasticity modulus of the material depending on the macrosample length: 1 – dependence of H_B , 2 – dependence of E .

The values of the Brinell hardness number of the material were measured at three different loads. As can be seen from the results presented in Fig. 4, an increase in the elasticity modulus affords a growth in the difference of the values of H_B measured at different static loads. This is connected with a nonlinear mechanical behavior of the high-modulus polymer material, when the parameters of a relaxation process are not constant and depend on the mechanical load or deformation.

The dynamic mechanical characteristics (storage modulus G' , loss modulus G'' , mechanical loss tangent $\text{tg}\delta$) were determined using two samples cut from different regions of the gradient material. The first sample with the length of 6 cm and the width of 1 cm contained sections 1–4 of the macrosample (Fig. 2). The elasticity modulus in it, according to equation (7), smoothly changed from 65 to 280 MPa. The second sample with the same sizes included sections 5–8, and its elasticity modulus changed from 280 to 712 MPa.

The dependences of moduli G' and G'' and $\text{tg}\delta$ on the temperature are demonstrated in Fig. 6. It is obvious that the storage modulus at the temperatures up to -60 °C takes on the high values equal to 1740 MPa. This is associated with the fact that in this temperature range the polymer is in a glassy state. Upon temperature rise from -60 to 150 °C, the storage modulus gradually reduces; at the same time, the storage modulus G' for the sample with the high values of E is essentially higher (curve 2) than that for the more low-modulus one (curve 1).

The temperature dependence of $\text{tg}\delta$ shows the presence of two maxima (Fig. 6c). An unsymmetrical shape of each of the maxima is caused by the gradient structure of the material, *i.e.*, the elasticity modulus of the samples is not a constant value and monotonously grows along their length. The first maximum is observed at the temperature of -38 °C. Its temperature is the same both for the high-modulus sample and for the low-modulus one and corresponds to devitrification of the fragments between cross-linked points. According to the results of calculation of the glass-transition points of linear fragments between cross-linked points of the material, which consist of poly(propylene glycol) chains, it is equal to -45 °C and is close to its experimental value. The calculation was performed using a Cascade program according to the following equation [2–5]

$$T_g = \frac{(\sum_i \Delta V_i)_{r,u}}{(\sum_i a_i \Delta V_i + \sum_i b_j)}, \quad (8)$$

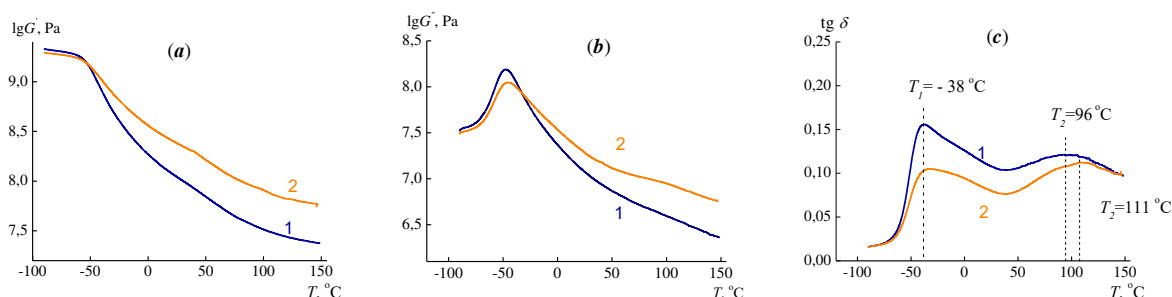


Figure 6. Dependences of the storage modulus (a), the loss modulus (b) and the mechanical loss tangent (c) on the temperature. The samples contained zones 1–4 (1) and 5–8 (2).

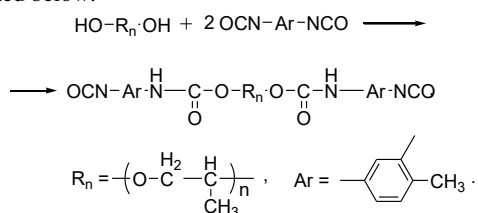
where $(\sum_i \Delta V_i)_{r,u}$ is the van der Waals volume of the repeating unit; a_i are the atomic constants connected with the energy of weak dispersion interaction, b_j are the constants connected with the energy of strong intermolecular interaction (dipole–dipole interaction, hydrogen bonds); and ΔV_i is the van der Waals volume of i atom.

The second maximum on the temperature dependence of $\text{tg } \delta$ is diffused. For the low-modulus sample, the temperature in it is equal to 96 °C, for the high-modulus one – to 111 °C. According to the previous results [12], the appearance of diffused extreme points on the temperature dependence of mechanical loss tangent is caused by the processes of microphase separation in the material and formation of microphases predominantly consisting of the isocyanurate rings and the epoxide oligomer included in the complex catalyst composition. It should be noted that at 150 °C the value of $\text{tg } \delta$ is close to 0.1. This indicates that at this temperature the gradient material retains the elastic properties and does not convert to an ordinary rubbery state.

Experimental

The following compounds were used as the reactants: poly(propylene glycol) with $M = 2000$ (**PPG-2000**) and the content of OH groups of 2.7%, $\rho^{25} = 0.99 \text{ g/cm}^3$, and $n_D^{30} = 1.4578$, prior to the synthesis it was evacuated at 100 °C for 2 h; 2,4-toluene diisocyanate (**2,4-TDI**) from ABCR GmbH & Co. KG with $M = 174.16$, bp = 121 °C/10 Hg mm, $\rho^{20} = 1.218 \text{ g/cm}^3$, and the content (mass fraction) of 2,4-isomer of 98%; D.E.R. 330 epoxy diene resin (**ER**) from Dow Chemical Company with the content of epoxy groups of 27.99–28.21% (defined by the direct method according to ISO 3001-1999) and $\rho^{25} = 1.16 \text{ g/cm}^3$; and dimethylbenzylamine (**DMBA**) with $M = 135.21$, $\rho^{20} = 0.91 \text{ g/cm}^3$, and bp = 180–183 °C.

To produce a gradient polymer material, a urethane prepolymer was synthesized preliminarily according to the published procedure [13] by the interaction of 2,4-TDI with PPG-2000 ($v_{\text{NCO}}: v_{\text{OH}} = 2.1:1$) at 70–75 °C. The reaction scheme is presented below:



The reaction course was controlled by the definition of the mass fraction of the NCO groups by back titration of a 0.2 M solution of dibutylamine in toluene with a 0.1 M solution of HCl in the presence of an indicator – bromophenol blue (according to ISO 11909-2007) as well as by measuring the refractive index of the reaction mixture n_D^{30} (Fig. 7). The heating was ceased in 4 h, when the mass fraction of the NCO groups reached 3.8%, which composes 53% of their conversion and is close to the value calculated based on the reaction scheme (58%).

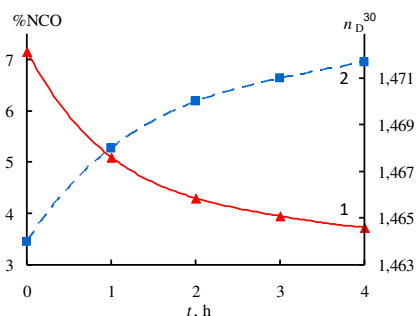


Figure 7. Dependences of changes in the mass fraction of the NCO groups (1) and the refractive index (2) on the reaction time during the synthesis of the urethane prepolymer based on PPG-2000 and 2,4-TDI.

The monolithic gradient polymer material with a gradual and continuous change of the elastic modulus along the length was produced on a semiautomatic laboratory casting unit which operation principle was described earlier [11] (Fig. 8).

For this purpose, two compositions were used that differed in the content of 2,4-TDI. The former mixture included 85 wt % of the resulting urethane prepolymer and 15 wt % of 2,4-TDI (component A); the latter contained 40 wt % of the same urethane prepolymer and 60 wt % of 2,4-TDI (component B). To accelerate the processes of cyclotrimerization and formation of isocyanurate structures, a DMBA/ER (1:20) complex catalyst was added to each mixture.

The choice of these compositions was dictated by the fact that the composition with the content of 2,4-TDI < 10 wt % has a relatively high viscosity, which complicates the control of outflow from capacities A2 and B2 (Fig. 8). The composition with the content of 2,4-TDI ≥ 70 wt %, after thermal curing imparts significant brittleness to a high-modulus part of the gradient material, which complicates further investigations of the mechanical properties.

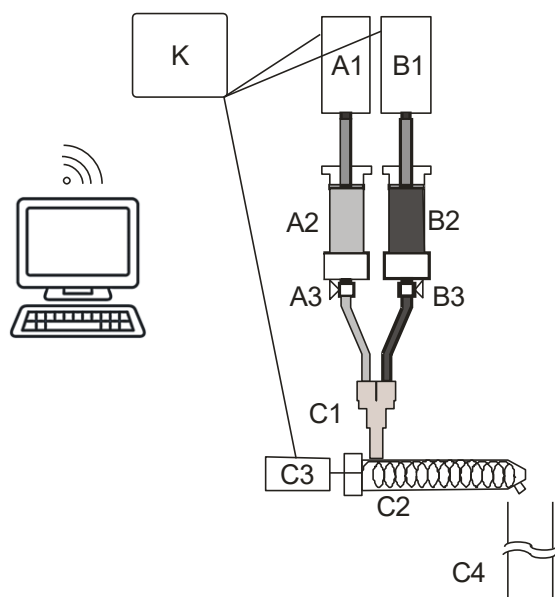


Figure 8. Schematic view of a unit for production of gradient polymer materials. A1 and B1 are the electromotors, A2 and B2 are the capacities for compositions, A3 and B3 are the isolation valves, C1 is the chamber of a blending unit, C2 is the dynamic blender, C3 is the electromotor of the blender, C4 is the mold for vertical casting, and K is the control unit.

Liquid compositions of variable formulation were charged into the corresponding capacities of the semiautomatic unit. The speed of outflow of each mixture was set and controlled using a programmed unit devised for control of the material synthesis according to the dependences depicted in Fig. 9. Two compositions were supplied with different rates into a single-screw extruder. After mixing, the composition was supplied into a casting mold in which the subsequent thermal processing afforded polycyclotrimerization, resulting in a network structure of the material. The kinetics and mechanism of formation of the isocyanate trimers are described in detail in review [14]; according to this reference, the predominant formation of isocyanurate structures can be accompanied by competitive formation of 2-oxazolidinone rings upon interaction of isocyanates with ER as well as other side processes. The reactions and products of interaction of ER with isocyanates and the compounds with an active hydrogen atom were reviewed in paper [15]. Taking into account that the total cocatalyst (ER) content in the catalytic system is low compared to the reaction mixture, the effect of the resulting side products on the morphology and properties of the gradient material obtained can be neglected.

The temperature curing in a casting mold was carried out in a stepwise manner from 60 to 120 °C each 20 °C at the seasoning time of 2 h. The geometrical dimensions of the resulting macrosample were as follows: length 15 cm, width 5 cm, and thickness 1 cm.

The macrosample was lined into 10 zones with the widths of 1.5 cm as is shown in Fig. 2.

The hardness tests were carried out on a TP-1 hardness testing machine with an indenter diameter of 4.95 mm at three static loads: 5, 10, and 15 kg. The measurements were carried out on the macrosample in the zones depicted in Fig. 2. The direction of the applied loading was perpendicular to that of the

sample rigidity change. The time for sample seasoning under the load composed 1 min. The Brinell hardness numbers were calculated by the following formula:

$$H_B = \frac{P}{\pi D h}, \quad (9)$$

where P is the load (kg), D is the indenter diameter (mm), and h is the indentation depth (mm).

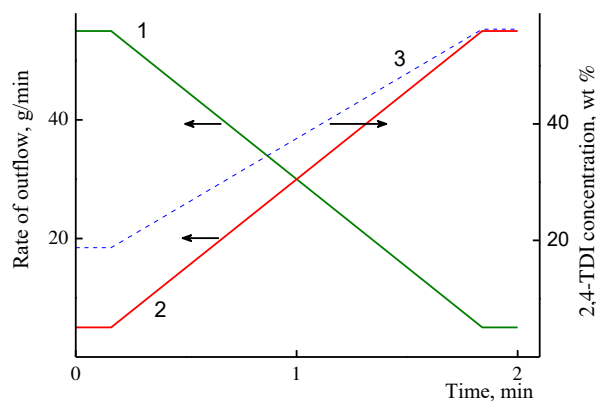


Figure 9. Time dependences of the rates of outflow of components A (1) and B (2) and a change in the concentration of 2,4-TDI in the mixture (3) during operation of the unit.

The mechanical properties upon uniaxial strain were measured on a Dubov–Regel unit for micromechanical tests. The samples with the dimensions of 4×4 mm and the thickness of 6 mm were cut from the microsamples. The rate of deformation upon measuring of the uniaxial compression curves composed $1.87 \cdot 10^{-1}$ mm/min. The stress–strain curves of the microsamples were measured in a direction perpendicular to the direction of a change in the macrosample rigidity. Since the sizes of the microsample sections were small (4×4 mm), these samples were considered to be single-modulus. The stress–strain curves were measured up to the strain value of 30%.

The dynamic mechanical characteristics (storage modulus G' , loss modulus G'' , and mechanical loss tangent $\text{tg} \delta$) of the samples cut from a block gradient material were defined on a MCR-302 rheometer (Anton Paar) in a twist/tension mode at the frequency of 1 Hz and the heating rate of 2 deg/min in the temperature range from –90 to 150 °C. The measurements were performed for two samples of the gradient material. The first sample with the length of 6 cm, the width of 1 cm and the thickness of 2 mm included sections 1–4 (according to Fig. 2). The second sample with the same sizes included sections 5–8.

Conclusions

The use of the semiautomatic laboratory casting unit for production of gradient materials testifies its effectiveness. The formation of gradient by mixing the compositions of different formulations occurs over a short period of time (2 min), which allows one to avoid gelling of a liquid mixture of the components. The following curing results in the gradient material of good quality without visible defects.

The gradient structure of the resulting material was confirmed experimentally. Thus, the Brinell hardness number increases along the length of the sample from 0.73 to

3.45 kg/mm² at the load of 15 kg. The elasticity modulus monotonously increases along its length upon material compression from 65 to 1106 MPa, *i.e.*, there is observed a gradual transition from an elastomer to a glassy polymer.

The programmed control of the material synthesis essentially simplifies its production and allows one to set different rates of the component feeding to the mold, where the following curing of the composition takes place, and to obtain the gradient material with the given change in the properties.

Corresponding author

* E-mail: andrey@ineos.ac.ru. Tel: +7(499)135-9398 (A. A. Askadskii)

References

1. A. A. Askadskii, Yu. I. Matveev, T. P. Matveeva, *Vysokomol. Soed., Ser. A.*, **1988**, *30*, 2542.
2. A. A. Askadskii, *Physical Properties of Polymers. Prediction and Control*, Gordon & Breach Publ., Amsterdam, **1996**.
3. A. A. Askadskii, *Russ. Polym. News*, **1999**, *4*, 34.
4. A. A. Askadskii, V. I. Kondraschenko, *Computational Materials Science of Polymers*, Moscow, Nauchnyi Mir, **1999** [in Russian].
5. A. A. Askadskii, *Computational Materials Science of Polymers*, Cambridge Int. Sci. Publ., Cambridge, **2003**.
6. S. Uemura, *Mater. Sci. Forum*, **2003**, 423–425, 1. DOI: 10.4028/www.scientific.net/MSF.423-425.1
7. B. Y. Wen, G. Wu, J. Yu, *Polymer*, **2004**, *45*, 3359. DOI: 10.1016/j.polymer.2004.03.023
8. A. A. Askadskii, L. M. Goleneva, K. A. Bychko, *Vysokomol. Soedin., Ser. A*, **1995**, *37*, 829.
9. A. A. Askadskii, L. M. Goleneva, *Macromol. Symp.*, **1996**, *106*, 9. DOI: 10.1002/masy.19961060104
10. A. A. Askadskii, L. M. Goleneva, *Proc. Int. Conf. on Fundamental Problems of Polymer Science*, Moscow, **1997**, p. 1 [in Russian].
11. A. A. Askadskii, L. M. Goleneva, K. A. Bychko, O. V. Afonicheva, *Polym. Sci., Ser. A*, **2008**, *50*, 781. DOI: 10.1134/S0965545X08070080
12. A. A. Askadskii, L. M. Goleneva, E. S. Afanas'ev, M. D. Petunova, *Rev. J. Chem.*, **2012**, *2*, 263. DOI: 10.1134/S2079978012030028
13. J. H. Saunders, K. C. Frisch, *Polyurethanes – Chemistry and Technology, Part 1: Chemistry*, Interscience Publ., New York, **1966**.
14. A. K. Zhitinkina, N. A. Shibanova, O. G. Tarakanov, *Russ. Chem. Rev.*, **1985**, *54*, 1104.
15. V. A. Pankratov, Ts. M. Frenkel', A. M. Fainleib, *Russ. Chem. Rev.*, **1983**, *52*, 576.